2010

Heat Rejection from R744 Near the Critical Point

Chieko Kondou
University of Illinois at Urbana-Champaign

Pega Hrnjak
University of Illinois at Urbana-Champaign

Heat rejection from R744 near the critical point

Chieko KONDOU[1]*, Pega HRNJAK[2]

[1]University of Illinois, Department of Mechanical Science and Engineering (ACRC), Urbana, IL, USA
E-mail;ckondo@illinois.edu

[2]University of Illinois, Department of Mechanical Science and Engineering (ACRC),
also Creative Thermal Solutions, Urbana, IL, USA
E-mail;pega@uiuc.edu

ABSTRACT

This paper presents experimental results of the study of heat rejection from CO_2 near the critical pressure: above it and below it, both in superheated and in two phase zone. The experimental data on HTC (heat transfer coefficient) and pressure drop in a horizontal smooth tube of inner diameter 6.1 mm at the pressure 5 to 7.5 MPa, enthalpy 280 to 450 kJ kg^{-1}, mass flux 100 to 250 kg m^{-2} s^{-1}, and heat flux 3 to 30 kW m^{-2} are provided. Experimental results are compared with correlations proposed for CO_2 when available and for other refrigerants. In the results, the occurrence of condensation in superheat zone was indicated from the experimental HTC much higher than correlation proposed for single phase turbulent HTC and tube wall temperature below the saturation temperature.

1. INTRODUCTION

In commercial refrigeration and some other applications of R744 systems, heat rejection in the vicinity of the critical pressure is the most important – in these conditions systems spend most of operating hours. So far, the most of the attention was given to the heat transfer in supercritical cooling even that is not the most frequent mode of heat rejection in CO_2 systems. In the case of subcritical operation which occurs much more frequently (typically below air/water temperatures of 22-25°C), heat rejection is with condensation. Even more, the heat transfer in superheat zone is much more important than for most other refrigerants, because the enthalpy change in superheat zone has the same order of magnitude as in phase changing zone. Therefore, understanding the heat rejection in superheat zone is very important for proper condenser (gas-cooler) sizing and design. However, the information about this process is very limited in open literature or non-existing for R744 to our best knowledge.

Fujii *et al*. (1978) measured condensation flow in two-phase zone of R11 and R113, and also Lee *et al*. (1991) measured R22 in horizontal smooth tubes. Fujii *et al*. measured temperature distribution of vapor in radial direction and proved that vapor is superheated even in two-phase zone. Those papers treat condensation as a condensation of superheated vapor and provide semi-rational empirical methods allowing for sensible heat rejection. This concept of condensation process proposed for two-phase zone could be extended in superheat zone.

Jiang *et al*. (2007) presented the experimental results on HTC of R404A and R410A in horizontal smooth copper-tubes of 9.4 and 6.2 mm inner diameter at reduced pressures of 0.8 and 0.9. They concluded the effect of pressure was not significant within their experimental conditions and correlation proposed for lower pressure by Cavallini *et al*. (2006) predicts well. Meanwhile, Koyama *et al*. (2008) presented the experimental results and modified correlation on void fraction, pressure drop and HTC of CO_2 condensation flow in horizontal micro-fin copper-tube of 5.67 mm equivalent inner diameter at 5 and 6 MPa. Their conclusion is that pressure drop and HTC decrease with rising pressure due to dense vapor and decreasing latent-heat. Activities of Hrnjak's group at ACRC cited at the end of the reference section were focused on condensation of CO_2 at low temperatures, where low stage of cascade systems operate. Their finding confirmed applicability of Cavallini's correlation at these conditions because of similarity of R22 and R744 thermophysical properties. However, heat rejection of superheat zone is not mentioned in any publication that is known to the authors.

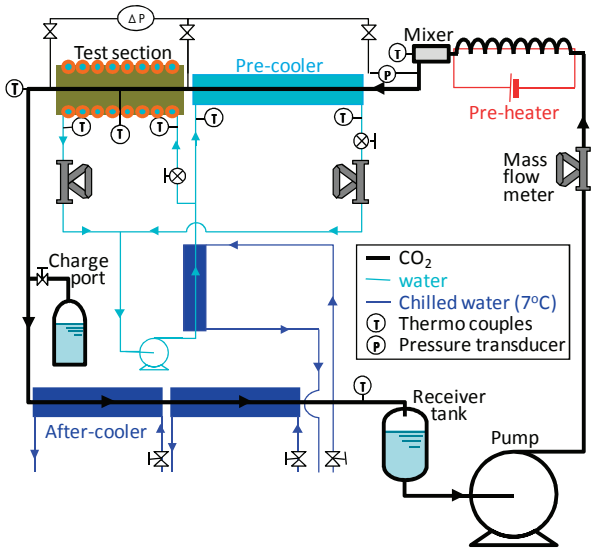

Figure 1: Experimental apparatus

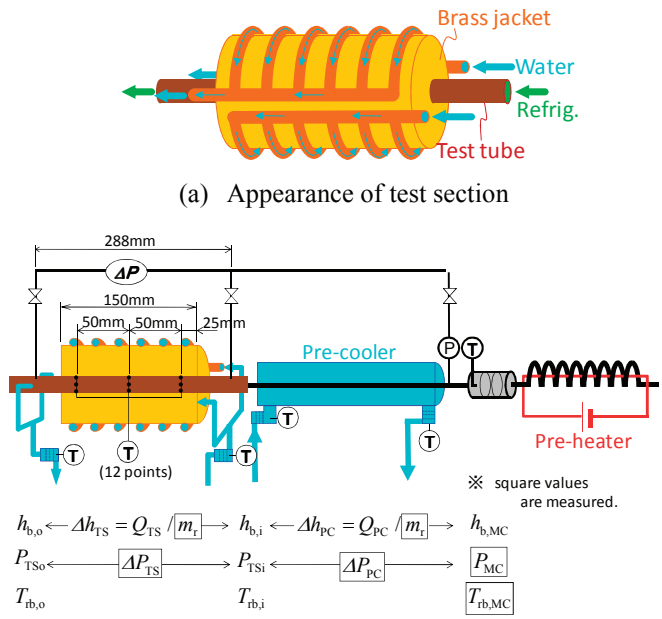

Figure 2: Test section and data reduction method

2. EXPERIMENTS

2.1 Apparatus

Figure 1 shows the schematic view of experimental apparatus which has CO_2, water and chilled water circuits. Components of CO_2 circuit are a gear pump, a coriolis-type mass flow meter, the pre-heater, the pre-cooler, the test section, after-coolers, and the receiver tank. In a mixer placed at the entrance of pre-cooler, bulk-mean-temperature and pressure of superheated vapor are measured. The pre-heater provides superheat in the mixer at least 5 K. The pre-cooler controls the inlet enthalpy of test section. The after-coolers control subcool in the receiver tank for keeping proper refrigerant flow rate. Pressure is controlled roughly by CO_2 charge amount and precisely by after-coolers.

2.2 Test Section

Figure 2 shows the schematic diagram of test section. The test section is a horizontal copper smooth tube with an inner diameter of 6.1 mm and outer diameter of 9.53 mm. 12 thermocouples are embedded into the top, bottom, right and left of the tube wall at three positions in axial direction. The test tube is covered with a thick brass jacket and thermal paste fills possible gap between them. Water flows through copper tubes wrapped outside of each brass segment. This approach provides cooling condition with almost uniform temperature. In addition, two holes of 1mm diameter are bored across the tube wall and capillary tubes are connected as pressure ports outside of the brass jacket. An active cooling length ΔZ_α is 150 mm and the length between pressure ports $\Delta Z_{\Delta p}$ is 288 mm.

2.3 Data Reduction Method

Figure 2 also shows the overview of data reduction method which begins with the enthalpy of superheated vapor in the mixer. Measured values are the bulk temperature and pressure of superheated vapor in the mixing chamber $T_{rb,MC}$ and P_{MC}, refrigerant mass flow rate m_r, differential pressures through the pre-cooler and test section ΔP_{PC} and ΔP_{TS}, inlet and outlet bulk temperature and mass flow rate of cooling water run through the pre-cooler $T_{H2O,PCi}$ $T_{H2O,PCo}$ $m_{H2O,PC}$ and test section $T_{H2O,TSi}$ $T_{H2O,TSi}$ $m_{H2O,TS}$, and 12 points of interior tube wall temperature T_{wi}. From $T_{rb,MC}$ and P_{MC}, the bulk enthalpy in mixing chamber $h_{b,MC}$ is determined with Refprop ver. 8.0. The enthalpy changes through each component Δh_{PC}, Δh_{TS} are obtained by water side heat balances.

$$\Delta h_{\mathrm{PC}} = Q_{\mathrm{PC}} / m_{\mathrm{r}} = \left(Q_{\mathrm{H2O,PC}} - Q_{\mathrm{gain,PC}}\right) / m_{\mathrm{r}} \tag{1}$$

$$Q_{\mathrm{H2O,PC}} = \left(T_{\mathrm{H2O,PCo}} - T_{\mathrm{H2O,PCi}}\right) m_{\mathrm{H2O,PC}} Cp_{\mathrm{H2O}} \tag{2}$$

$$\Delta h_{\mathrm{TS}} = Q_{\mathrm{TS}} / m_{\mathrm{r}} = \left(Q_{\mathrm{H2O,TS}} - Q_{\mathrm{gain,TS}}\right) / m_{\mathrm{r}} \tag{3}$$

$$Q_{\mathrm{H2O,TS}} = \left(T_{\mathrm{H2O,TSo}} - T_{\mathrm{H2O,TSi}}\right) m_{\mathrm{H2O,TS}} Cp_{\mathrm{H2O}} \tag{4}$$

where, $Q_{\mathrm{gain,PC}}$ and $Q_{\mathrm{gain,TS}}$ are experimentally determined (calibrated) heat input from ambient air through the insulation. The averaged heat flux on interior tube wall q_{wi} is,

$$q_{\mathrm{wi}} = \left(Q_{\mathrm{H2O,TS}} - Q_{\mathrm{gain,TS}} - Q_{\mathrm{cond}}\right) / \left(d_{\mathrm{i}} \cdot \pi \cdot \Delta Z_{\alpha}\right) \tag{5}$$

where, Q_{cond} is the conduction heat from outside of cooling brass jacket. The central refrigerant temperature of test section T_{rb} is defined as an arithmetic mean of inlet and outlet bulk temperatures $T_{\mathrm{rb,i}}$ $T_{\mathrm{rb,o}}$ which are found from each pressure P_{TSi} P_{TSo} and enthalpies $h_{\mathrm{b,i}}$ $h_{\mathrm{b,o}}$. Hence, the definition of averaged heat transfer coefficient α_{r} is,

$$\alpha_{\mathrm{r}} = q_{\mathrm{wi}} / \left(T_{\mathrm{rb}} - T_{\mathrm{wi}}\right) \tag{6}$$

The averaged HTC and pressure drop are measured at refrigerant mass flux G_{r} from 100 to 250 kg m^{-2}s^{-1}, pressure P from 5.0 to 7.5 MPa, the heat flux q_{wi} from 3 to 30 kW m^{-2}, bulk enthalpy in test section h_{b} from 250 to 480 kJ kg^{-1}.

3. EXPERIMENTAL RESULTS AND DISCUSSION

3.1 Experimental Results and Categorization of Heat Rejection Process

Figure 3 (a) and (b) show the experimental results at 6 and 7MPa for q_{wi} = 10 kW m^{-2} and G_{r} = 150 kg m^{-2} s^{-1}. Bottom horizontal axis is bulk-mean enthalpy of refrigerant h_{b} and upper is bulk-mean vapor quality x_{b}. Upper graphs show bulk-mean refrigerant temperature of test section at the inlet $T_{\mathrm{rb,i}}$ and outlet $T_{\mathrm{rb,o}}$, the average of 12 points interior tube wall temperatures T_{wi}, and the averaged heat flux on interior tube wall q_{wi}. Graphs at the middle show the averaged HTC α_{r} in the test section and predictions by three correlations. Bottom graphs show the average pressure drop gradient $\Delta P/\Delta Z$ and newly proposed prediction method to be described.

Change in $T_{\mathrm{rb,i}}$ and $T_{\mathrm{rb,o}}$ from right to left indicate first presence of sensible heat removal (desuperheating) as temperature decreases and then latent heat at the saturation temperature. Here, the temperature is bulk mean value. In two-phase zone, HTC is compared with correlations proposed for condensation flow of other refrigerants by Haraguchi *et al*. (1994), Cavallini *et al*. (2006). In superheat and subcool zone, data are compared with a correlation proposed for single-phase turbulent of variable property gases by Petukhov (1970). Cavallini's correlation of two-phase zone condensation shows best agreement in literatures as Jiang et al. (2007) concluded from their experimental results of R404 A and R410 A.

3.2 Condensation in Superheat Zone

As shown in Fig. 3, experimental HTC is well predicted by Petukhov's correlation around the bulk enthalpy h_{b} = 450 kJ kg^{-1}, when tube wall temperature T_{wi} is over the saturation. As interior wall temperature T_{wi} reaches the saturation temperature about h_{b} = 430 kJ kg^{-1}, experimental HTC starts deviating from the Petukhov's correlation (increasing) and eventually HTC shows the same value as condensation HTC in two-phase zone at the vapor quality x_{b} = 1.0. This situation indicates presence of condensation, caused by the tube wall temperature being below the saturation temperature. This condensation in superheat zone is more pronounced at 6 MPa than 7 MPa because of larger ratio of latent to sensible heat.

Figure 4 (a) shows the schematic of temperature profile measured by Fujii *et al*. (1978). They horizontally measured temperature distribution of vapor flow across middle plane of a tube and proved core vapor flow is superheated even in the two-phase zone. This interpretation can be sufficiently extended to superheat zone; although bulk temperature is still superheated, refrigerant flow facing the tube wall enters ahead the two-phase zone.

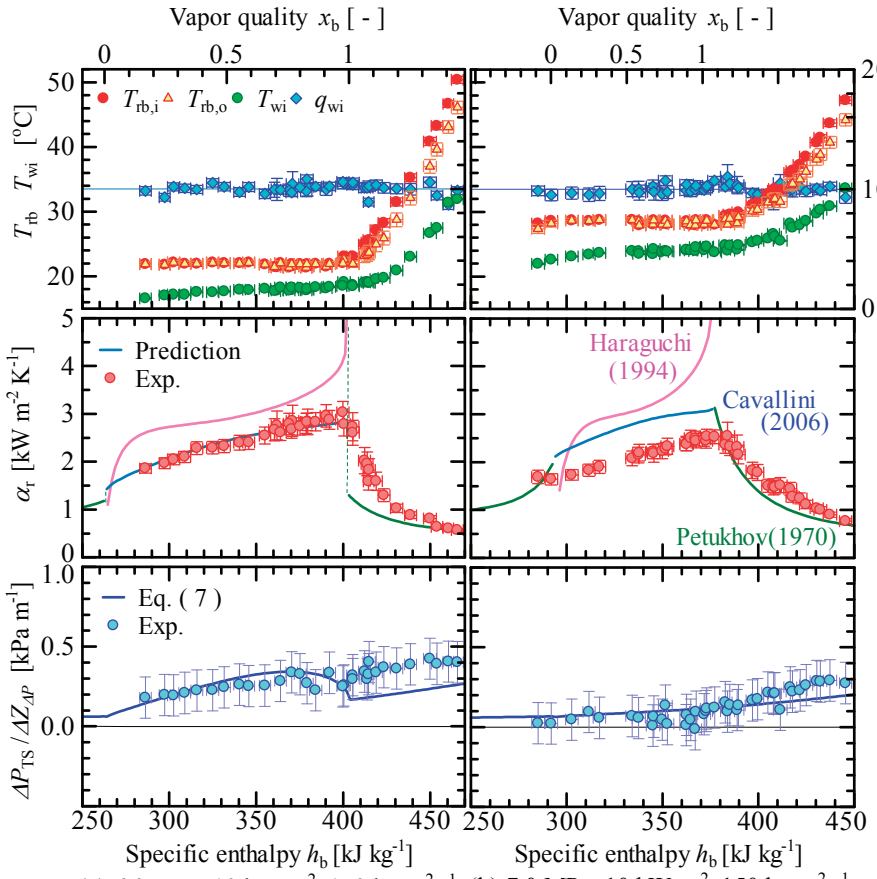

(a) 6.0 MPa, 10 kW m^{-2}, 150 kg m^{-2}s^{-1} (b) 7.0 MPa, 10 kW m^{-2}, 150 kg m^{-2}s^{-1}

Figure 3: Specifications of experimental results

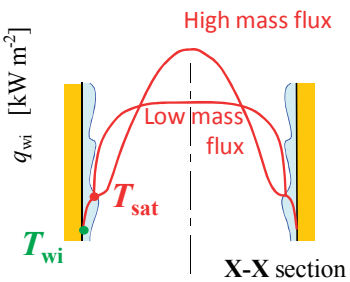

(b) temperature profile
Fujii *et al*. (1978)

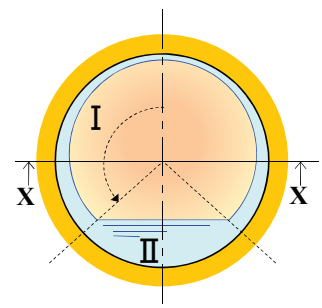

(a) physical model
Haraguchi *et al*. (1994)

Figure 4: Physical model of condensation flow in smooth tube

3.3 Effects of Mass Flux, Heat Flux, and Pressure on HTC

Figure 4 (b) shows physical model on condensation flow of low mass flux which proposes dominant HTC region I and another region filled by liquid layer II. In the region I, the body force convection caused by falling thin liquid film on HTC combined with forced convection caused by vapor velocity. In the region II, forced convection of the slow liquid layer on tube wall and vapor flowing on liquid surface effects on HTC. However, the HTC of the region II is presumed relatively small to region I. Effects of mass flux, heat flux, and pressure on HCT are discussed with this physical model.

Figures 5 (a), (b), and (c) show experimental HTC for various mass fluxes, heat fluxes, and pressures respectively compared to correlations by Cavallini and Petukhov. As shown in Fig 5 (a), HTC increases with increasing mass flux. Obviously Cavallini's correlation shows very good fidelity.

As shown in Fig 5 (b), at high superheats experimental HTC is well predicted by Pethukov's correlation. Experimental data demonstrated more gradual merging between Petukhov's and Cavallini's correlations then correlations themselves. Petukhov's correlation deviates more at higher heat fluxes and closer to saturation. The reason is that the higher heat flux causes tube wall temperature to decreases and reaches saturation temperature earlier. Thus, high heat flux causes the superheated vapor to start condensation earlier. In the two-phase zone, experimental HTC increases with increasing heat flux and the increment plateaus at 15 kW m^{-2}. On the other hand, the correlation shows that HTC decreases. According to Nusselts't film wise condensation theory, HTC decreases because growing liquid film works as a heat resistance. However, this theory proposed for laminar free convection condensation assumes quiescent vapor and ignores the forced convection by flowing superheated vapor. From the experimental HTC, it is presumed that heat transfer of turbulent flow condensation is slightly prompted by heat flux but limited.

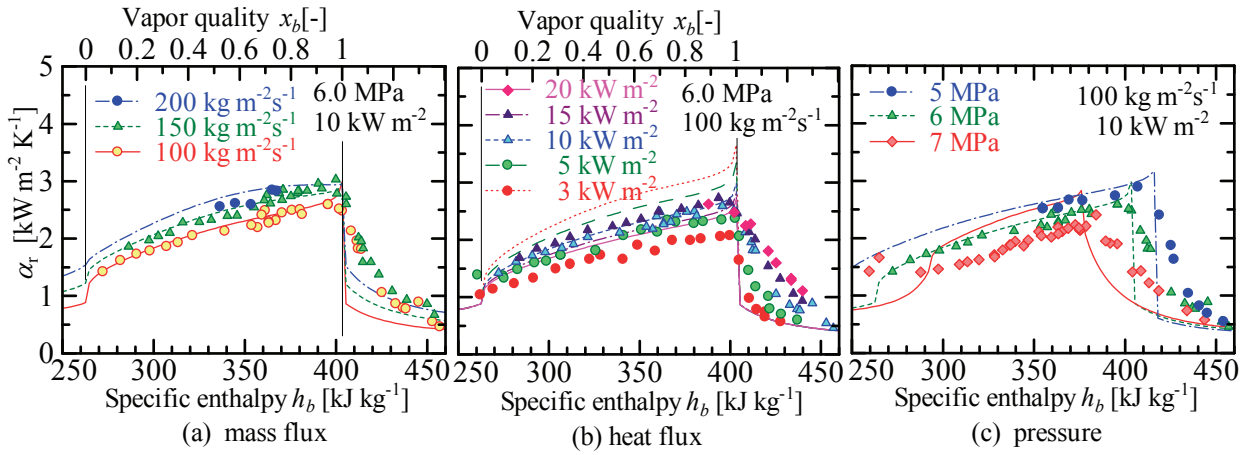

Figure 5: Effects of mass flux, heat flux, and pressure on HTC (symbols; experimental HTC, curves; prediction)

As shown in Fig 5 (c), experimental HTC decreases monotonically with pressure; however the correlation deviates from experimental HTC and increases at 7 MPa. That is not surprising because the experimental data is beyond the range of the Cavallini's correlation and it is really surprising how well it works at all. For further discussion, following elements should be noted: 1) Thicker liquid film due to lower liquid density and higher Prandtl number. 2) Low vapor velocity. 3) Temperature distribution in liquid film and flowing vapor caused by higher specific heat. 4) Balance of smaller latent heat and larger sensible heat. 5) Waves on the liquid surface due to lower surface tension. Those complex phenomena affect the subcritical heat transfer.

3.3 Heat Rejection and Pressure Drop around the Critical Point

Figure 6 shows effect of pressure on HTC and pressure drop gradient at enthalpy 320 to 360 kJ kg^{-1}. As shown in Fig. 6 (a), experimental HTC constantly decrease with rising pressure and turn to increase at 7.3 MPa then turn to decrease at 7.5 MPa. On the other hand, as shown in Fig 6 (b), experimental pressure drop follows similar development but transitions occur at slightly different pressures.

Above presented results have some common points with previous research on film-wise condensation on vertical cold wall. Fujii and Watabe (1987) are derived Nusselt number from governing equations with stream functions and also confirmed experimentally with subcritical CO_2 and water vapor. According to their conclusions, Nusselt's film wise condensation theory can be extended and HTC decreases constantly until 7.3 MPa then starts increasing toward the critical point. Although the experimental results are indistinct, HTC shows turning point about 7.3 MPa and this agrees their conclusions. However, the reason why HTC has its peak at 7.5 MPa (just above the critical pressure) is still unknown. On the other hand, Ishihara *et al.* (2002) observed behavior of falling liquid of subcritical CO_2. According to their visualization, the behavior changes to random chevron-shaped wave from laminar or periodic gentle wave at 7.2 MPa due to decreasing surface tension. Also, experimental pressure drop gradient has the obvious

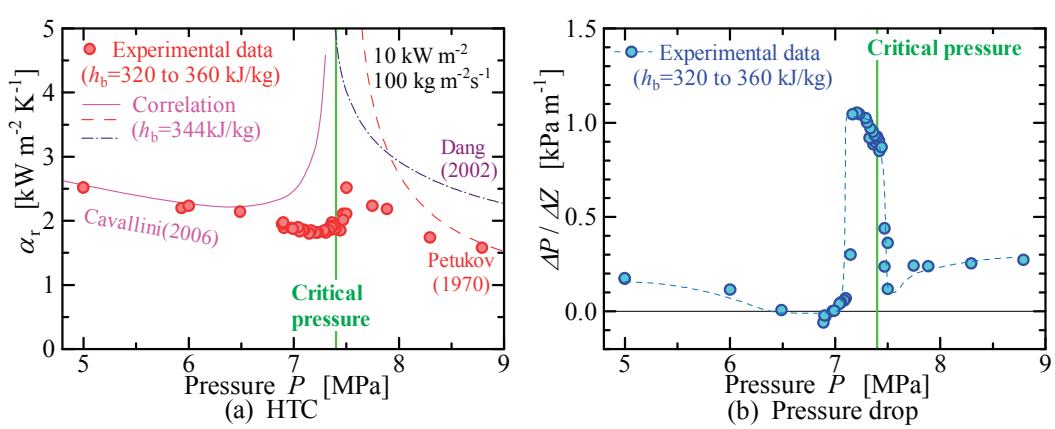

Figure 6: Effect of pressure on HTC and pressure drop across the critical point

turning point at 7.2 MPa and it could be explained by momentum dissipation at that complex liquid surface. About 7.5 MPa just above the critical pressure, Petukhov's correlation shows extremely high HTC because of thermal properties. Compared to this, Dang and Hihara (2007) proposed the prediction method for transcritical gas cooling as appended with the dotted line in Fig. 6 (a). Their method considers strong fluid property distribution in tube radius near the pseudo-critical temperature. Although the prediction is not perfect in vicinity of the critical point Dang and Hihara predict better than Petukhov's correlation. As shown in the top chart of HTC at7.5 MPa in Fig. 7, the maximum HTC of Dang and Hihara's prediction is much closer to experimental HTC; however, the calculation does not converge when film temperature is close to pseudo-critical temperature.

3.4 Effect of Superheat Zone Condensation on Sizing of Cross-finned Tube Heat Exchangers

Figure 7 shows serious of experimental results plotted on P-h diagram. As shown in this figure, condensation in superheat zone is more important at higher reduced pressure. Higher compressor discharge temperature increases the importance of the condensation in the superheat zone in sizing of heat exchanger: both higher HTC and greater LMTD are potential for reducing the size of the heat rejecting coil.

Figure 8 shows an example focused on a cross-flow fin tube type condenser. There is concern that the heat resistance of air side could reduce the effects of good refrigerant side heat transfer. The air side HTC, surface area

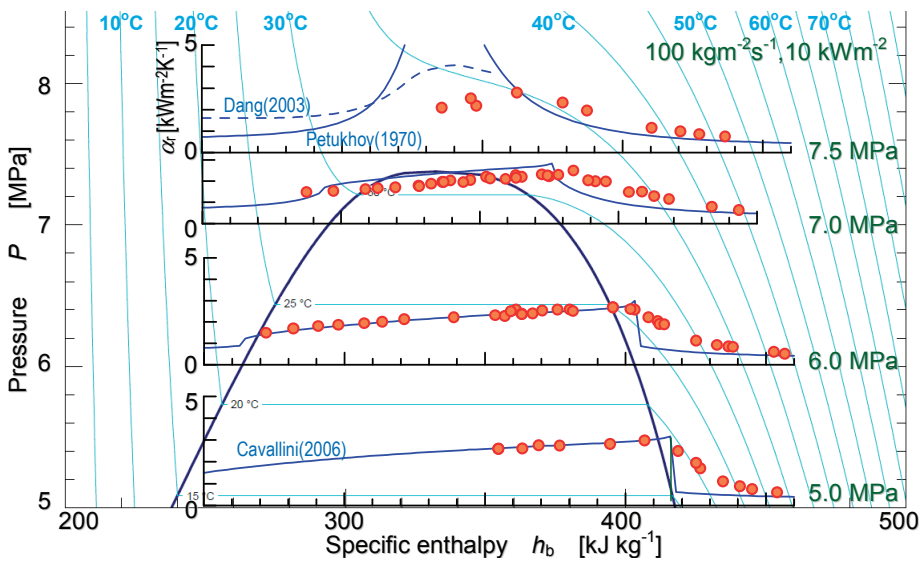

Figure 7: Experimental HTC on P-h diagram

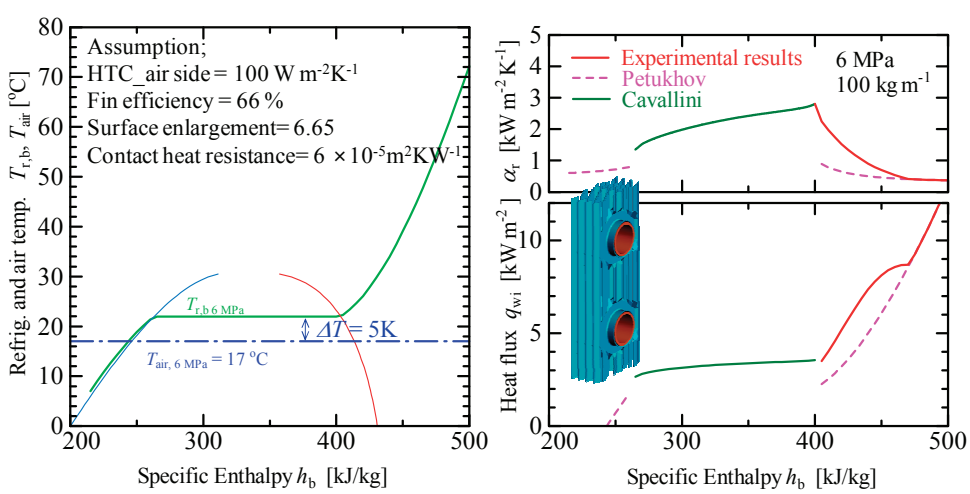

Figure 8: Effect of condensation in super heat zone on cross-finned tube heat exchangers

enlargement, fin efficiency, and contact heat resistance is assumed as shown is the left box of Fig. 8. The heat conduction through the fin caused by refrigerant temperature gradient is ignored. Furthermore, the air temperature is assumed below 5 K of refrigerant saturation temperature at 7 MPa which is typical condition of spring and autumn. Refrigerant side HTC is assumed to have the value as shown by solid curve in upper right chart in Fig. 8 based on experimental results at 6 MPa 100 kg $m^{-2}s^{-1}$ 10 kW m^{-2} and it is compared to the calculation results using Petukhov's correlation. The calculation results are shown in bottom right chart in Fig 8. The heat flux on interior tube wall taking into account superheat zone condensation is plotted with solid line and if ignoring it is plotted with dashed line. The difference indicates the potential for reduction of the heat exchanger size.

3.5 Modified Correlation for Pressure Drop Gradient

Figure 3 shows the experimental pressure drop gradient in the chart at the bottom. The experimental results are compared with correlation plotted with solid line. Koyama *et al*. (2008) proposed an empirical correlation for CO_2 flow condensation in micro-fin tube. As a trial, their friction factor replaced to Colburn's correlation of smooth tube and Colburn's correlation is extended to superheat and subcool zone. However, at 7MPa, the gentle peak of pressure drop gradient in two-phase zone disappeared at 7 MPa. The reason might be in very slow vapor flow due to dense vapor which reduces slip between liquid and vapor flow and causes flow regime very quiet stratified flow. This is also expected from lowest point around 7 MPa as shown in Fig. 6 (b). Therefore, for prediction of pressure drop at 7 MPa, Maltinelli-Nelson's correlation of two-phase multiplier proposed for the critical point is applied. Here, the modified correlation is summarized in equations (7) to (11).

$$\frac{\Delta P}{\Delta Z} = \left\{ \left(\frac{dP_{\mathrm{M}}}{dZ} \right) \Delta Z_{\alpha} + \left(\frac{dP_{\mathrm{F}}}{dZ} \right) \Delta Z_{\Delta P} \right\} \Big/ \Delta Z_{\Delta P} \tag{7}$$

$$dP_{\mathrm{M}} = \begin{cases} \text{Two-phase zone:} \quad G_{\mathrm{r}}^{2} \left\{ \left[\dfrac{x^2}{\xi \rho_{\mathrm{V}}} + \dfrac{(1-x)^2}{(1-\xi)\rho_{\mathrm{L}}} \right]_{\mathrm{inlet}} - \left[\dfrac{x^2}{\xi \rho_{\mathrm{V}}} + \dfrac{(1-x)^2}{(1-\xi)\rho_{\mathrm{L}}} \right]_{\mathrm{ontlet}} \right\} \\ \text{Else:} \quad G_{\mathrm{r}}^{2} \left(1/\rho_{\mathrm{inlet}} - 1/\rho_{\mathrm{outlet}} \right) \end{cases} \tag{8}$$

$$\left(\frac{dP_{\mathrm{F}}}{dZ} \right) = x \Phi_{\mathrm{V}}^{2} \left(\frac{dP_{\mathrm{F}}}{dZ} \right)_{\mathrm{V}} + (1-x) \Phi_{\mathrm{L}}^{2} \left(\frac{dP_{\mathrm{F}}}{dZ} \right)_{\mathrm{L}} \tag{9}$$

$$\begin{cases} 0.8 < P/P_{\mathrm{crit}} \le 0.97 : \Phi_{\mathrm{V}} = \left(X_{\mathrm{tt}} + 1 \right)^{0.9}, \Phi_{\mathrm{L}} = \left(1 + 1/X_{\mathrm{tt}} \right)^{0.9} \\ P/P_{\mathrm{crit}} \le 0.8 : \Phi_{\mathrm{V}} = 1.0 + 1.7 F_r^{0.1} X_{tt}^{-0.55}, \Phi_{\mathrm{L}} = 1.0 + 1.8 F_r^{0.1} X_{tt}^{-0.9} \end{cases} \tag{10}$$

$$\left(\frac{dP_{\mathrm{F}}}{dZ} \right)_{\mathrm{V}} = 0.046 Re_{\mathrm{V}}^{-0.2} \left(\frac{G_{\mathrm{r}}^{2} x^2}{2 d_{\mathrm{i}} \rho_{\mathrm{V}}} \right), \quad \left(\frac{dP_{\mathrm{F}}}{dZ} \right)_{\mathrm{L}} = 0.046 Re_{\mathrm{L}}^{-0.2} \left[\frac{G_{\mathrm{r}}^{2} (1-x)^2}{2 d_{\mathrm{i}} \rho_{\mathrm{L}}} \right] \tag{11}$$

In two-phase zone, above correlation satisfactorily agrees with experimental results, however, prediction results are lower than experimental results in superheat zone. This indicates that secondary flow and condensing liquid film affects pressure drop and counting those is necessary for accurate prediction superheat zone pressure drop.

CONCLUSIONS

This paper presents results of heat rejection transfer and pressure drop in round tube near critical CO_2. These results contain in addition to supercritical gas cooling and condensation the data for condensation in superheat zone. To our best knowledge this is the first experimental data for these phenomena. The conclusions are following:

- In the SH zone, experimental HTC is higher than the prediction for single-phase turbulent HTC because of condensation of superheated vapor.
- In two-phase zone, Cavallini's correlation agrees well with experimental HTC up to 6MPa; however slightly deviates at 7 MPa.
- Experimental HTC at 344 kJ kg^{-1} increases with increasing mass flux and heat flux. The HTC decreases with rising pressure until 7.3 MPa and turn to increase until 7.5MPa, then decreases again.

- Experimental pressure drop at 344 kJ kg^{-1} decreases with rising pressure until 7 MPa and suddenly jumps up at 7.2 MPa, then drops down at the critical pressure.
- Modified correlation for prediction of pressure drop is proposed; however, it needs further development. New correlation for heat transfer is underway.

NOMENCLATURE

	Symbols			**Subscripts**
d_i	Inner diameter	(m)	r	refrigerant
g	gravitational acceleration	(m s^{-2})	H2O	water
h	specific enthalpy	(J kg^{-1})	b	bulk
q	heat flux	(W m^{-2})	wi	interior tube wall
m	mass flow rate	(kg s^{-1})	TSi	test section inlet
G	mass flux	(kg $m^{-2}s^{-1}$)	TSo	test section outlet
P	pressure	(Pa)	PCi	pre-cooler inlet
T	temperature	(^oC)	PCo	pre-cooler outlet
Q	heat transfer rate	(W)	MC	mixer
Z	tube length	(m)	α	active heat transfer length
α	heat transfer coefficient	(W $m^{-2}K^{-1}$)	ΔP	length between pressure ports
ρ	density	(kg m^{-3})	M	momentum change term
μ	viscosity	(Pa s)	F	friction term
ξ	void fraction	(-)	gain	heat leak from ambient air
Fr	Froude number = $G_r / \{ g\, d_i \rho_V (\rho_L - \rho_V) \}^{0.5}$	(-)	cond	conduction heat
Re_V	vapor Reynolds number = $G_r\, x\, d_i / \mu_V$	(-)	V	vapor
Re_L	liquid Reynolds number = $G_r (1 - x)\, d_i / \mu_L$	(-)	L	liquid
Φ	two-phase multiplier	(-)	crit	critical point of pressure
X_{tt}	Lockhart–Martinelli parameter for turbulent = $(1/x - 1)^{0.9} (\rho_V / \rho_L)^{0.5} (\mu_L / \mu_V)^{0.1}$	(-)		

REFERENCES

Fujii, T., Honda, H., Nozu, S., and Nakarai, S., 1978, Condensation of superheated vapor inside a horizontal tube, *Heat Transfer - Japanese Research*, 4 (3), pp. 1-48.

Lee, C. C., Teng, Y. J., and Lu, D. C., 1991, Investigation of condensation heat transfer of superheated R-22 vapor in a horizontal tube, *Proceeding of World Conference Experimental Heat Transfer, Fluid Mechanics, and Thermodynamics*., pp. 1051-1057.

Jiang, Y., Mitra, B., Garimella, S., and Andresen, C., 2007, Measurement of condensation heat transfer coefficients at near-critical pressures in refrigerant blends, *Transactions of ASME J. Heat transfer*, 129, pp. 958-965.

Cavallini, A., Del Col, D., Doretti, L., Matkovic, M., Rossetto, L., Zilio, C., and Censi, G., 2006, Condensation in horizontal smooth tubes: a new heat transfer model for heat exchanger design, *Heat Transfer Engineering*, 27 (8) 31-38.

Koyama, S., Kondou, C., and Kuwahara, K., 2008, An experimental study on condensation of CO_2 in a horizontal micro-fin tube, *12th International Refrigeration and Air Conditioning Conference at Purdue*, paper no. 2322.

Lemmon, E. W., Huber, M. L., and McLinden, M. O., 2007. Reference fluid thermodynamic and transport properties-REFPROP ver.8.0, National Institute of Standards and Technology, Boulder, CO, USA.

Haraguchi, H., Koyama, S., Fujii, T., 1994, Condensation of refrigerants HCFC 22, HCFC 134a and HCFC 123 in a horizontal smooth tube (2nd report; Proposals of empirical expressions for local heat transfer coefficient), *Transactions of the Japanese Society of Mechanical Engineers* (B), 60 (574) pp.2117-2124 (in Japanese).

Petukhov, B. S., 1970, Heat transfer and friction in turbulent pipe flow with variable physical properties, Advances Heat Transf., *Academic Press*, Orland, 6, p.523, 536.

Fujii, T., and Watabe, M., 1987, Laminar film condensation in the subcritical region – Gravity controlled condensation, *Transactions of the Japanese Society of Mechanical Engineers* (B), 53 (490), pp. 1801-1806 (in Japanese).

Ishihara, I., Mori, H., and Matsumoto, R., 2002, Behavior of condensate of carbon dioxide in subcritical region,

Transactions of the Japanese Society of Mechanical Engineers (B), 68 (671), pp. 1878-1883 (in Japanese).

Dang, C., and Hihara, E., 2003, Cooling heat transfer of supercritical carbon dioxide: A new correlation for heat transfer coefficient and effect of lubricant oil, *Transactions of the Japan Society of Refrigerating and Air Conditioning Engineers,* 120, (2) pp. 175-183 (in Japanese).

Kim, Y. J., Jang, J., Hrnjak, P. S., and Kim, M. S., 2008, Adiabatic horizontal and vertical pressure drop of carbon dioxide inside smooth and microfin tubes at low temperatures, *Journal of Heat Transfer*, 130:11, Nov.

Kim, Y. J., Jang, J., Hrnjak, P. S., and Kim, M. S., 2009, Condensation heat transfer of carbon dioxide inside horizontal and vertical pressure smooth and microfin tubes at low temperatures, *Journal of Heat Transfer*, 131:2, .

Jang, J., and Hrnjak, P. S., 2002, Condensation of carbon dioxide at low temperatures, *Proceedings of International Institute of Refrigeration Conference on Natural Refrigerants*, Guangchou, 64-74.

Jang, J., and Hrnjak, P. S., 2003, Flow regimes and heat transfer in condensation of carbon dioxide at low temperatures, *Proceedings of International Conference on Heat Transfer, Fluid Mechanics and Thermodynamics 2003*, Victoria Falls.

Zilly, J., Jang, J., and Hrnjak, P. S., 2003, Condensation of carbon dioxide at low temperatures in micro-finned horizontal tubes, *Proceeding of International Institute of Refrigeration*, Washington D.C.

Park, C. Y., and Hrnjak, P. S., 2009, CO_2 condensation heat transfer and pressure drop in multi-port microchannels, *3rd IIR Conference on Thermophysical Properties and Transfer Processes of Refrigerants*, Boulder, CO, June 23-26, 2009.

Zilly, J., J. Jang, and Hrnjak, P. S., 2003, Condensation of CO_2 at low temperature inside horizontal microfinned Tubes, *ACRC Report No. CR-49, Mar. 2003*.

Jang, J., and Hrnjak, P. S., 2004, Condensation of CO_2 at low temperatures, *ACRC Report CR-56, June 2004*.

ACKNOWLEDGEMENT

We are grateful for financial support from the Air Conditioning and Refrigeration Center (ACRC) at the University of Illinois and technjcal (instrumentation and original facility) from Creative Thermal Solutions (CTS).